JOURNAL OF SOLID STATE CHEMISTRY **76**, 229–234 (1988)

Stability and Lattice Pressure in Complex Perovskite Superconductors

H. OESTERREICHER

Department of Chemistry, University of California, San Diego,
La Jolla, California 92093

Communicated by J. M. Honig, June 17, 1988

Spatial and electronic criteria for stability of complex perovskite superconductors are analyzed. We describe rules according to which complex perovskite materials are not likely to be obtained when simple perovskites can be built from some of the elements in question. For materials such as $YBa_2Cu_3O_x$, one finds two qualitatively different Cu stackings, namely a symmetric one (^{s}Cu between Ba planes) and an asymmetric one (^{a}Cu stacked between Ba and Y). ^{a}CuO adjusts to the available space by buckling, while ^{s}CuO is planar. This results in increased lattice pressure on ^{s}Cu, leading to oxidation beyond Cu^{2+}, i.e., to hole creation, with increasing x, which is initially localized on ^{s}Cu. We suggest that this is the origin of an independent modification with $T_s \sim 60$ K. When holes can penetrate to ^{a}Cu, $T_s \sim 90$ K. These arguments can be generalized to include materials such as $Bi_2Sr_2Ca_{n-1}Cu_nO_x$. Strategies for searching for new materials are outlined.

Introduction

After the discovery of several high transition temperature (T_s) superconductor families based on CuO (e.g., $(LaSr)_2CuO_x$, $YBa_2Cu_3O_x$, $CaSr_2Bi_2Cu_2O_x$, or $Ca_2Ba_2Tl_2Cu_3O_x$; see Refs. (*1–8*)) questions of their stability and important structural features have become of interest for understanding and designing new materials. We attempt here a crystal chemical analysis which may serve as an initial step for this purpose. We first describe structural results of high T_s and related materials, and then analyze them with regard to space filling and electronic considerations. We finally compare results and extrapolate into the future.

Results

Table I contains a representative sampling of structural features of high T_s and related materials, together with their schematic stacking sequences. To analyze their space filling, we present, in Table II, ionic diameters of the elements in question. Ionic diameters are also shown in Fig. 1 as a function of valency and used to rationalize their stability. Classical perovskites, such as the prototype $CaTiO_3$, are composed of 2+ and 4+ ions. The simple cubic perovskite stacks a $M^{2+}O$ layer (B site) on top of a $M^{4+}O_2$ layer (A site) which is turned by 90° (*ab* diagonal). The sum of the M^{2+} and O^{2-} diameters, denoted as $dM^{2+}O$, should be equal to the distance $\sqrt{2}\,dM^{4+}O$. In this respect, it is customary to use a tolerance factor t for stability of perovskites,

$$t = \frac{d_B + d_0}{\sqrt{2}(d_A + d_0)} = \frac{dBO}{\sqrt{2}\,dAO},$$

where d_A and d_B are ionic diameters for the two metals in question and $d_0 = 2.80$ Å, the

0022-4596/88 $3.00

TABLE I

STRUCTURAL DATA ON HIGH T_s AND RELATED MATERIALS

Material	Symmetry	Lattice dimensions[a] a_0	b_0	c_0 (Å)	Stacking
$La_{1.8}Sr_{0.2}CuO_4$	Tetr.	3.78		13.23	Cu La La Cu
$YBa_2Cu_3O_7$	Orthorh.	3.83	3.89	11.67(3.89)	Cu Ba Cu Y Cu Ba Cu
$YBa_2Cu_3O_6$	Tetr.	3.86		11.81(3.94)	
$LaBa_2Cu_3O_7$	Tetr.	3.92		11.76(3.92)	Cu Ba Cu La Cu Ba Cu
$CaSr_2Bi_2Cu_2O_x$	Orthorh.	5.41(3.83)	5.44(3.85)	30.78	Cu Ca Cu Sr Bi Bi Sr Cu
$CaSr_2Bi_2Cu_3O_x$	Orthorh.	5.40(3.82)	5.46(3.86)	38.2	Cu Ca Cu Ca Cu Sr Bi Bi Sr
$CaBa_2Tl_2Cu_2O_x$	Tetr.	5.44(3.85)		29.55	Cu Sr Cu Ba Tl Tl Ba Cu
$Ca_2Ba_2Tl_2Cu_3O_x$	Tetr.	5.40(3.82)		36.25	Cu Sr Cu Sr Cu Ba Tl Tl Ba Cu
$NaCa_2Nb_3O_{10}$	Tetr.	7.73(3.87)		(28.98)	Nb Ca Nb Ca Nb Na Nb
$Bi_4Ti_3O_{12}$	Orthorh.	5.41(3.83)	5.45(3.85)	32.84	Ti Bi Bi Ti Bi Ti Bi Ti
$Y_2Cu_2O_5$	Orthorh.	15.72(3.93)	12.76(4.15)	8.21	
$YCuO_3$	Hex.	5.31(3.75)		13.02	
$BaCuO_2$	Cub.	18.26			
$In_2Cu_2O_5$	Orthorh.	24.62(3.1)	10.54(3.51)	3.27	
$BaPbO_3$	Cub.*	4.27			
$BaBiO_3$	Cub.*	4.35			

[a] Values in parentheses correspond to primitive perovskite cell dimensions. Values with asterisks denote averaged cubic dimensions of lower symmetry material.

TABLE II

SPATIAL PARAMETERS OF METAL–O DISTANCE

Metal ion	*dM* (Å)	*dMO* (Å)[a] *A*	*B*
Cu^+	1.9	4.7	(6.6)
Cu^{2+}	1.4	4.2	(5.9)
Cu^{3+}	1.1	3.9	
Ca^{2+}	2.0	(3.4)	4.8
Sr^{2+}	2.3	(3.6)	5.1
Ba^{2+}	2.7	(3.9)	5.5
Pb^{2+}	2.4	(3.7)	5.2
Y^{3+}	1.9		4.7
La^{3+}	2.3	(3.6)	5.1
In^{3+}	1.6	(3.1)	4.4
Tl^{3+}	1.9	(3.3)	4.7
Bi^{3+}	2.4	(3.7)	5.2
Na^+	1.9	(3.3)	4.7
K^+	2.7	(3.9)	5.5
Rb^+	3.0	(4.1)	5.8
Ti^{4+}	1.4	4.2	
Ce^{4+}	2.0		4.8
Pb^{4+}	1.7		4.5

[a] Diameter metal ion +2.8 Å (O^{2-}) for *A* and *B* sites, respectively. *A* and *B* sites differ by a factor of $\sqrt{2}$.

diameter of O^{2-}. Generally, ΔH is the more exothermic the closer t is to unity (values range (*9*) from −81 kJ for $CaTiO_3$ to −152 kJ for $BaTiO_3$). For $CeBaO_3$, $t = 0.81$, which lies toward the lower limit of structural tolerance for this compound. Nevertheless, the combination of a 2+ and a 4+ ion appears to make this a relatively stable perovskite, as reflected in the fact that so far no Ce analog to $YBa_2Cu_3O_x$ has been found (*6*, *8*), but that at this composition, $CeBaO_3$ can be one component in the phase diagram. The possible deleterious influence of the extra electron on Ce as compared to Y appears to be of no importance for "Ce $Ba_2Cu_3O_x$," as valency tailoring through partial Ce substitution by Na did not (*7*) stabilize the $YBa_2Cu_3O_x$-type structures but produced $CeBaO_3$ as a component.

Aspects of the structure of $YBa_2Cu_3O_x$ are schematically shown in Fig. 2 and Table I. We distinguish in the stacking between a symmetric (^{s}Cu stacked between planes of

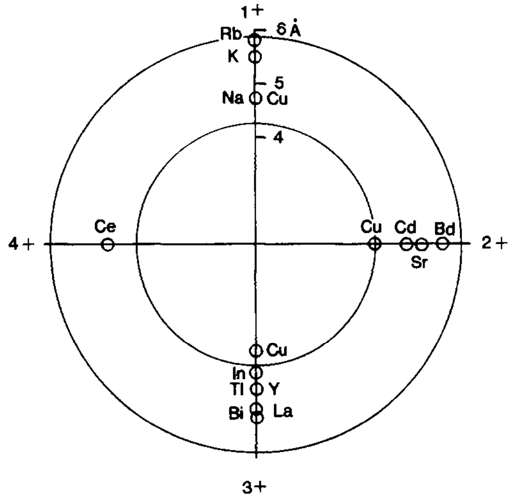

FIG. 1. Ionic space filling dMO (in Å) as a function of valency. Components from east and west quadrants (2+ 4+) should form simple valency perovskites. 1+ 3+, 1+ 4+, and 3+ 4+ combinations should have the potential to form complex perovskites. Two circles have been drawn with radii $dCu^{2+}O$ and $\sqrt{2}\,dCu^{2+}O$ to indicate the spatial requirements for other atoms.

Ba, also referred to as chain Cu) and an asymmetric Cu (^{a}Cu stacked between Ba and Y or plane Cu). The stability of $YBa_2Cu_3O_{6.5}$ (see Ref. (*4*) for literature compilation) derives from good *ab* diagonal stacking between Cu^{2+} and Ba^{2+}, with $t = 0.93$ for these metals. Y atoms are inserted in an unusual manner which results in diagonal stacking with a component along *c* (*bc* diagonal). YO can therefore act as a buffer for space mismatch. The BaO unit cell diagonal defines the dimension along the *a* and *b* axes at 3.9 Å. For $dCu^{2+}O = 4.18$ Å, space filling has to be accomplished by partial buckling and bond compression. $dCu^{2+}O$ survives roughly along *c* with 4.16 Å and for the buckled ^{a}CuO bond. ^{s}Cu, however, is under increased lattice pressure along *b* because of the absence of buckling. The requirements for Y space filling are 4.80 Å. This, without buckling, would have to be accommodated (Fig. 2) along a *bc* diagonal at a distance $(3.89^2 + 3.36^2)^{1/2} = 5.14$ Å. This value is much too large but the observed O buckling leads to accommodation if we allow for the O–O contact distance as $(3.89^2 + 2.8^2)^{1/2} = 4.79$ Å. This indicates quite generally a diameter requirement of 2.0 Å for an ion in the *bc* diagonal with a cell edge of 3.9 Å (fixed by BaO and CuO) and O–O contact. Y^{3+}, Ca^{2+}, Cd^{2+}, Na^{+} are typical elements fulfilling this requirement. The orthorhombic splitting then establishes hard sphere contact between Y and O along the diagonal marked by the shorter (*a*) axis on a rigid sphere model. In these respects, $YBa_2Cu_3O_7$ is a marvel of successful space filling.

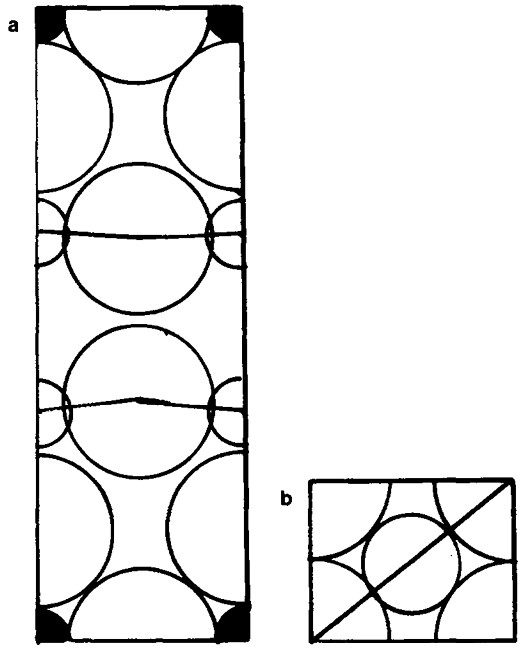

FIG. 2. (a) Representation of space filling in $YBa_2Cu_3O_7$ along *b* and *c*. The large circles represent O^{2-}, the small filled circles represent $^{s}Cu^{3+}$, the small open circles represent $^{a}Cu^{2+}$. ^{s}Cu is under increased lattice pressure resulting in initial localization of Cu^{3+} on this site (with $T_s \sim 60$ K). Distances are ^{s}Cu–^{a}Cu: 4.16 Å, ^{a}Cu–^{a}Cu: 3.36 Å along *c*. (b) Representation of space filling in $YBa_2Cu_3O_7$ along *a*/2 and *c*. The large partial circles are O^{2-}; the smaller circle is Y^{3+}. Distances are O–O, 2.8 Å along *c*; O–Y–O, 4.7 Å along *ac* diagonal.

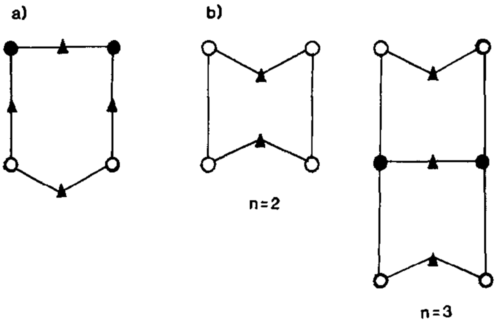

FIG. 3. (a) Schematic representations of $YBa_2Cu_3O_7$ increased lattice pressure on ^sCu or "chain" site (filled circle) over the one of ^aCu "plane" site (open circle, while triangles represent oxygen). This leads to ^sCu valencies >2+ and initial chain site superconductivity with $T_s \sim 60$ K followed by plane site superconductivity with $T_s \sim 90$ K with increasing x for $YBa_2Cu_3O_x$. The horizontal Cu–Cu distance is 3.89 Å; the vertical one is 4.15 Å. (b). Schematic diagram for $Bi_2Sr_2Ca_{n-1}Cu_nO_x$ of buckling of Cu–O bonds (Cu are represented by round symbols, O by triangles). The filled round symbols represent ^sCu which is under higher lattice pressure, due to the absence of pronounced buckling on account of symmetry. We assume that ^sCu sites are responsible for $T_s \sim 120$ K, by comparison with ^aCu with $T_s \sim 80$ K.

We now attempt to explain in terms of spatial requirements (lattice pressure) the presence of two plateaus at $T_s \sim 60$ and 90 K in $YBa_2Cu_3O_x$ (*10, 11*). For this, we invoke a smaller bond distance Cu–O–Cu for ^sCu compared to ^aCu, as ^sCu–O is not buckled (Fig. 3). This should preferentially oxidize ^sCu to 3+ and generate $T_s \sim 60$ K. This tendency for chain site ^sCu to assume the 3+ state for $x = 7$ is also brought out by band structure calculations (*12*). When the plane site ^aCu also obtains sufficient valency (>2), it becomes superconducting, with $T_s \sim 90$ K. The c axis trends also corroborate this behavior. The shrinkage of c with x reflects the successive straightening of the buckled Cu plane sites as the Cu valency increases. An accelerated decrease happens just before the second plateau in T_s is reached (*4*). The implication for T_s (and x) of symmetric and asymmetric stacking of Cu can be carried to related compounds such as $Bi_2Sr_2Ca_{n-1}Cu_nO_x$ (*13*) and $CaBa_2Tl_2Cu_2O_x$ (*14*).

For $CaSr_2Bi_2Cu_2O_x$, the cell dimensions are roughly fixed by the BiO and SrO space filling (Table I), presumably also with buckling of CuO bonds. For $CaBa_2Tl_2Cu_2O_x$, dTlO is considerably smaller compared to dBiO, and more severe CuO buckling can be assumed in this case. Generally, we expect that only the larger divalent ions can form complex perovskites with Cu in higher valency states (a similar situation is obtained with early transition metals as shown in Table I). This condition is somewhat relaxed with $CaSr_2Bi_2Cu_2O_x$ and $CaBa_2Tl_2Cu_2O_x$ or $Ca_2Ba_2Tl_2Cu_3O_x$. We note, however, that the Bi (large ion) compound forms with the relatively smaller Sr while the Tl (smaller ion) compound forms with the larger Ba. This appears again to indicate a principle of averaged space filling. In both cases (BiSr and TlBa) the averaged size for dMO is ~5.1 Å. For InBa, the average size would be 4.9 Å, making analogs such as $Sr_{n+1}Ba_2In_2Cu_{n+2}O_x$ a possibility.

Discussion

Criteria for selection of elements in synthesizing complex perovskite materials that incorporate CuO include valence and size. The valence criterion appears relatively complex. A straightforward aspect can be stated negatively: no complex perovskite is stable whenever simple "valence perovskites" can be built from the elements in question (East–West components in Fig. 1). An example is the absence (*6, 8*) of $CeBa_2Cu_3O_x$, due to the stability of $CeBaO_3$ which fulfills the basic requirement of 2+ and 4+ valency of the two metals in question. Concerning size, perovskites can be considered as a marriage of partners whose radii differ by a factor of $\sqrt{2}$. This is exemplified by the selection of large 2+ ions in forming ceramic superconductors (Fig. 2).

These defect perovskites, however, illustrate a second structural principle, namely an O defect layer which is built by OO contact along c, and a bc diagonal spacer atom with an ionic diameter of ~2 Å. For this, elements in the periodic table diagonal such as Na^+, Ca^{2+}, Y^{3+} are suitable. The latter two have amply demonstrated their usefulness, and Na^+ has shown a potential for large homogeneous regions (*7*) in $Y_{1-y}Na_y Ba_2Cu_3O_x$.

For mixed valent components in two crystallographic sites such as Cu in $YBa_2 Cu_3O_x$, the spatial requirements (lattice pressures) can be different on these sites. This can lead to preferential hole creation (or mixed valence) on one site. As a result, stepwise increases in T_s as a function of O doping can be expected in some cases. This is indeed found for $YBa_2Cu_3O_x$ where we postulate the T_s ~ 60 K to be related to initial 3+ oxidation (holes) on ^{s}Cu. At higher x, holes also penetrate to ^{a}Cu ("plane Cu") and generate T_s ~ 90 K. The importance of ^{a}Cu in the T_s ~ 90 K phase has been indicated through substitutional studies (*21*), where it was shown that Zn^{2+} substitutes for ^{a}Cu, strongly reducing T_s, while the smaller Ga^{3+} substitutes for ^{s}Cu, having only a small effect on T_s.

A similar situation is obtained with compounds such as $Bi_2Sr_2Ca_{n-1}Cu_nO_x$. In this case with $n = 2$ (Fig. 3), only ^{a}Cu is found and T_s ~ 80 K. For $n = 3$, one plane of ^{s}Cu is inserted and T_s ~ 120 K. We can assume that for $n > 3$, no major changes in T_s should occur, as this does not lead to qualitatively new spatial arrangements. $T_s(x)$ for $n = 3$ should show only one rise to the maximum T_s value because ^{s}Cu oxidizes first and the subsequent oxidation of ^{a}Cu will be masked. We note that partial Zn^{2+} substitution would preferentially occur on ^{a}Cu; this should, therefore, not have a pronounced effect on T_s ~ 120 K for $n = 3$, but does influence T_s ~ 80 K for $n = 2$. We further note that only ^{s}Cu should give strong changes in T_s as a function of lattice parameters, as ^{a}Cu can readjust through buckling. This should also lead to strong pressure dependences of T_s in the relevant cases. we can assume that the T_s ~ 60 K phase in $RBa_2Cu_3O_x$ should then lead to increased or decreased T_s values, depending on the size of R. This appears to be indicated by the T_s ~ 56 K value in $LaBa_2Cu_3O_x$, compared to T_s ~ 61 K for $YBa_2Cu_3O_{6.6}$ (*22*).

The series of compounds with increasing n is reminiscent of the situation with early transition metal compounds such as the Aurivillius (*19*) or Ruddlesden-Popper series (*20*). We note, however, the distinct difference between the stacking (Table I) in $Ca_2Ba_2Tl_2Cu_3O_x$ and $Bi_4Ti_3O_{12}$ (Aurivillius phase representative). In both cases, there exist double layers of Bi or Tl, respectively. However, in the Aurivillius phases, these double layers are joined directly by transition metals while in $Ca_2Ba_2Tl_2Cu_3O_x$, they are joined by Ba layers. There is a complete analogy between early and late transition metal analogs in the stacking of $NaCa_2 Nb_3O_{10}$ and $YBa_2Cu_3O_7$, although the O coordination is different. As a mixture of asymmetric and symmetric Cu stacking appears to induce mixed Cu valence in $YBa_2 Cu_3O_x$, materials such as $NaCa_2Nb_3O_{10}$ may have a potential for high T_s when suitably doped such that Nb would be in a low d electron configuration. An intriguing question remains concerning the difference in O coordination of Bi or Tl (e.g., six coordinated in $CaSr_2Bi_2Cu_2O_x$) and Y (eight coordinated in $YBa_2Cu_3O_x$). This difference obviously is unrelated to the lone pair on Bi, as Tl also has this coordination, or to size, as $dTl^{3+} \sim dY^{3+}$. One possible difference is the potential d electron involvement with Y. In any case, the energetic differences between these stacking variations should not be strong; it might be possible also to obtain Y analogs of the $CaSr_2Bi_2 Cu_2O_x$-type structures.

Generally, we note that in addition to enforcing the basic structural features, metals such as Ba increase the oxidizing power on Cu, due to their low electronegativity and large size. Also, the buckling of CuO bonds will not only be dictated by space filling needs but will reflect the pressure of antibonding orbitals, by bending bonds and partially converting antibonding into nonbonding electrons.

Conclusion

In conclusion, we note that complex perovskites are stable in those cases where components cannot form simple perovskites, due to size or electronic limitations. In $R\mathrm{Ba_2Cu_3O}_x$ compounds, one can understand the presence of two superconducting modifications (with $T_s \sim 60$ and 90 K, respectively) as a result of the stepwise creation with x of d holes in Cu through different lattice pressures at the two crystallographic sites in question (^{s}Cu, ^{a}Cu). The difference in T_s between analogs such as $\mathrm{Bi_2Sr_2Ca}_{n-1}\mathrm{Cu}_n\mathrm{O}_x$ with $n = 2$ and 3 can also be explained by the presence of ^{s}Cu (with diminished buckling of CuO) only in the latter. In order of increasing T_s one finds ^{s}Cu one-dimensional (1D) ($\mathrm{YBa_2Cu_3O}_x$, $T_s \sim 60$ K), ^{a}Cu 2D ($\mathrm{YBa_2Cu_3O}_x$ similar to $\mathrm{Bi_2Sr_2CaCu_2O}_x$ with $T_s \sim 80$ to 90 K), and ^{s}Cu 2D ($\mathrm{Bi_2Sr_2Ca_2Cu_3O}_x$ with $T_s \sim 120$ K). The principle of size averaging appears to stabilize some complex stacking variations. This principle, together with plausible stacking sequences, should be helpful in discovering new high T_s materials.

References

1. J. G. Bednorz and K. A. Muller, *Z. Phys. B* **64,** 189 (1986).
2. R. M. Hazen, L. W. Finger, R. J. Angel, C. T. Prewitt, H. K. Mau, C. G. Hadidiacos, P. H. Hor, R. L. Meng, and C. W. Chu, *Phys. Rev. B* **35,** 7238 (1987).
3. R. J. Cava, B. Batlogg, R. B. van Dover, D. W. Murphy, S. Sunshine, T. Siegrist, J. P. Remeika, E. A. Rietman, S. Zahurak, and G. P. Espinosa, *Phys. Rev. Lett.* **58,** 1676 (1987).
4. J. D. Jorgenson, M. A. Beno, D. G. Hinks, L. Soderholm, K. Z. Volin, R. L. Hitterman, J. D. Grace, I. K. Schuller, C. U. Segre, K. Zhang, M. S. Kleefisch, *Phys. Rev.* **36,** 3608 (1987).
5. R. M. Hazen, *et al.*, preprint.
6. H. Oesterreicher and B. Higgins, *Mater. Lett.* **6,** 254 (1988).
7. A. Fartash and H. Oesterreicher, *Solid State Commun.* **66,** 39 (1988).
8. M. Smith, A. Fartash, J. Zhang, and H. Oesterreicher, *Mater. Lett.* **6,** 208 (1988).
9. E. Takayama-Muromachi and A. Navrotsky, *J. Solid State Chem.* **72,** 244 (1988).
10. R. J. Cava, B. Batlogg, C. H. Chen, E. A. Rietman, S. M. Zahurak, and D. Werder, *Phys. Rev. B* **36,** 5694 (1987).
11. M. G. Smith, J. Zhang, and H. Oesterreicher, *Mater. Res. Bull.* **23,** 563 (1988).
12. L. A. Curtiss, T. O. Brun, and D. M. Gruen, *Inorg. Chem.* **27,** 1421 (1988).
13. R. Ramesh, G. Thomas, S. Green, C. Jiang, Yu Mei, M. L. Rudee, and H. L. Luo, preprint.
14. Z. Z. Sheng and A. M. Hermann, *Nature (London)* **332,** 138 (1988).
15. M. Dion, M. Ganne, and M. Tournoux, *Mater. Res. Bull* **16,** 1429 (1981).
16. M. Dion, M. Ganne, M. Tournoux, and J. Ravez, *J. Chim. Miner.* **21,** 92 (1984).
17. A. J. Jacobson, J. T. Lewandowski, and J. W. Johnson, *J. Less-Common Met.* **116,** 137 (1986).
18. M. Goudrand and J. C. Joubert, *Rev. Chim. Miner.* **24,** 33 (1987).
19. B. Aurivillius, *Ark. Kemi* **1,** 499 (1949); **5,** 39 (1952).
20. S. N. Ruddlesden and P. Popper, *Acta Crystallogr.* **10,** 538 (1957), **11,** 54 (1958).
21. G. Xiao, *et al.*, *Nature (London)* **332,** 236 (1988).
22. H. Oesterreicher, B. Higgins, and A. Fartash, *Mater. Res. Bull,* in press.